

Impact of Two Connection Types on the Behavior and Losses of a Steel Hotel Building Under Strong Winds in Mexico

David De Leon & Gerardo Lazcano

**International Journal of Civil
Engineering**

ISSN 1735-0522

Int J Civ Eng
DOI 10.1007/s40999-017-0238-z



 Springer

Your article is protected by copyright and all rights are held exclusively by Iran University of Science and Technology. This e-offprint is for personal use only and shall not be self-archived in electronic repositories. If you wish to self-archive your article, please use the accepted manuscript version for posting on your own website. You may further deposit the accepted manuscript version in any repository, provided it is only made publicly available 12 months after official publication or later and provided acknowledgement is given to the original source of publication and a link is inserted to the published article on Springer's website. The link must be accompanied by the following text: "The final publication is available at link.springer.com".

Impact of Two Connection Types on the Behavior and Losses of a Steel Hotel Building Under Strong Winds in Mexico

David De Leon¹ · Gerardo Lazcano¹

Received: 20 December 2016 / Revised: 27 May 2017 / Accepted: 12 June 2017
© Iran University of Science and Technology 2017

Abstract Two connection types are examined under a life-cycle point of view, for a regular framed steel hotel building located in Mexico under a strong wind hazard, to compare their cost-effectiveness and provide practical recommendations. Although FEMA has fragility curves for housing facilities under strong winds, there are no curves for medium height or tall buildings like the one used to illustrate the formulation. The critical connections were identified through a series of preliminary analyses of the ten stories building, which were performed under scenario wind velocities, and a detailed finite-element model was used to evaluate the connection limit state and the failure probability at both levels: the connection and the overall building. The cost-effectiveness of bolted and welded connections was examined, as alternative designs, through the calculation of the expected life-cycle cost. Envelope damages are explicitly considered as façade components and windows are usually damaged and cause important losses. In addition, the potential loss of contents is assessed as a consequence of water infiltration after the building envelope is damaged, and the expected business interruption losses, from the repairs required, are included in the cost analysis. The correlation coefficient between wind velocity and rainfall intensity, given the occurrence of a hurricane, is calculated and incorporated on the simulation of rainfall intensity. Recommendations to mitigate losses

are proposed in terms of the fragilities found and the cost of mitigation measures. It is shown that low-cost improvements, on the façade and windows anchorage conditions, strongly reduce the expected losses and the cost–benefit of these measures decreases as the building importance increases.

Keywords Steel connection types · Expected life-cycle cost · Wind hazard · Water infiltration · Fragility curves

1 Introduction

Many buildings located on zones with high wind hazard, usually hotel facilities, have been damaged under strong hurricanes in Mexico [1, 2]. In addition, engineers are wondering what type of steel connection is appropriate for a given hazard type and intensity. The fragile fractures of welded connections in the Northridge earthquake [3] highlighted the uncertainties about the proper selection and cost-effectiveness of connection types between many options: bolted, welded, a combination of both, shear, seated on an angle, brackets, rigid, semi-rigid, moment-resting, end plates, gusset plates, cover or side plates, dog bones, among others.

Several researchers have studied some of them through either lab tests or analytical models. As an example, several moment resisting connections have been studied under seismic excitation [4]. End plates have been tested under cyclic loading [5]. Several authors proposed a procedure to test spot-welded steel connections under static and impact loadings [6]. Other researchers claim that the actual semi-rigid stiffness of joints that are neither pinned nor embedded connections should be considered for the calculation of its reliability [7]. Extended end-plate connections have

✉ David De Leon
dleon@uaemex.mx; daviddeleonescobedo@yahoo.com.mx

Gerardo Lazcano
lazcanogerardo@hotmail.com

¹ Faculty of Engineering, Department of Structural Engineering, Universidad Autonoma del Estado de Mexico, Estado de Mexico, Toluca 50130, Mexico

been experimentally studied [8]. The cyclic behavior of welded steel beam-to-column connections was studied under cycles of constant and variable amplitude [9]. The Research Council on Structural Connections recommends specifications for high strength bolts [10]. Unstiffened extended plates have been analyzed to provide design recommendations [11]. Bolted brackets have been tested under cyclic loading [12].

A book that has become a classical on the topic of ductile design of steel structures shows the behavior of typical steel connections [13]. In China, some specifications have been developed for steel structural members and connections [14]. Gusset plate connections on rectangular hollow braces have been analyzed through numerical simulation [15]. Connections with brackets have been studied through nonlinear analysis [16].

A probabilistic optimization procedure has been applied to the analysis of a space truss. A number of procedures on earthquake engineering have served as a guide, with the corresponding adaptations, to do applications on wind engineering, as in a recent paper where seismic demands have been assessed for moment resisting frames. Monte Carlo simulation techniques have also been applied to assess the reliability of bolted connections [17]. Some works have studied the behavior of steel angles filled with concrete under dynamic loading [18]. An improved link to column connection was proposed to improve the behavior of eccentrically braced frames [19]. In addition, a procedure to assess the vulnerability of tall buildings with steel plate shear wall, x-braced, and moment frame was proposed to predict progressive collapse on the building.

Recently, gusset plates have been tested as joints of steel braces with eccentricity [20].

In a previous paper [21], a scheme was proposed to assess the cost/benefit of alternative steel connections for a building under seismic hazard. Research interest has focused on adapting reliability and expected life-cycle cost techniques to assess the effectiveness of steel structures design proposals [22]. However, since some time ago, the structural design has been benefited by the probability-based formats [23–25].

To assess the lifetime performance of the building, the cost–benefit assessment appears to be an adequate tool to measure the cost-effectiveness of each alternative and select the one that best combines the structural safety and cost. Here, the alternatives are the steel connections and the selection criterion is the minimum expected life-cycle cost.

In this paper, the concept of the expected life-cycle cost is extended and applied to steel connections of buildings exposed to wind hazard in Mexico, to examine alternative connections, and provide recommendations for its selection and ultimately update the current design code. The cost and

reliability of the alternative steel connections are put in perspective, because although the welded connection is more expensive than the bolted one, its structural reliability is higher and therefore, reduces the failure future cost. Therefore, there is an optimal reliability level for a given wind hazard exposure and a certain structural type. Inspired on the FEMA criteria developed for low rise homes exposed to strong winds [26], fragility curves are derived for the considered building, extending those criteria to include the typical damages on medium and high rise buildings when a hurricane occurs.

In addition, original estimations of losses are derived from the building failure probability and the likelihood of partial damages, like contents damage due to water infiltration and losses due to business interruption. The correlation between hurricane winds and rainfall intensity, given a hurricane, is included into the calculations.

Existent values in the literature are taken to measure the uncertainty on some parameters that play an important role on the buildings and connections responses under wind loading [25, 29]. In addition, structural reliability concepts, extreme value distribution, and correlation theory [27] are applied to calculate the building annual failure probability and the expected cost of water infiltration.

A regular-geometry framed steel building, assumed to be constructed in Cancun, Mexico, a site under strong wind hazard, is considered for a typical structural type and height. The building is analyzed through a nonlinear static response analyses, under six scenario maximum wind velocities and the maximum responses on the critical connections are characterized in terms of these wind velocities.

The maximum wind velocity, as previously obtained for Cancun [28], has a Gumbel probability distribution and is used to calculate the forces on the building. Then, the failure probability is calculated throughout the use of the connection structural capacities and the application of Monte Carlo simulation, as ahead explained.

The failure mechanism is considered as the occurrence of connection failure combination at six critical joints that would produce the failure at the first three stories, on the right bay area of the building if the wind forces are acting from left to right. The opposite holds for wind acting from right to left. Then, the expected life-cycle cost is obtained by adding the initial cost to the future cost: the product of the failure probability and the updated cost of failure consequences.

The consequences include potential fatalities, injuries, loss of contents and finishing, and the loss of profit due to business interruption, due to the repair period. To explore the impact that might have the loss magnitude on the selection of connection type, several levels of consequences cost are considered.

The results may contribute to the performance-based design of connections for steel buildings under strong wind hazard in Mexico.

2 Proposed Procedure

2.1 Expected Life-Cycle Cost

The proposed procedure is based on the assessment of the expected life-cycle performance of preselected connections and scenario of mitigation measures, including the modeling of the building and connections and the calculation of inherent costs. This is done to compare connection types and, later on, mitigation strategies. The well-known expected life-cycle cost $E(C_L)$ [24, 33] is expressed:

$$E(C_L) = C_i + E(C_C), \quad (1)$$

where C_i is the initial cost and $E(C_C)$ is the present value of the expected failure consequences:

$$E[C_C] = [C_D]P_f, \quad (2)$$

where P_f is the annual failure probability of the building.

The failure consequences are composed by the costs of the building repair/replacement, potential fatalities and injuries, and the loss of profit like rentals due to business interruption (during repairs) C_{D1} :

$$C_D = PVF[C_{D1}]. \quad (3)$$

Here, PVF is the present value factor required to update the costs $[C_{D1}]$ according to the following function [34]:

$$PVF = [1 - \exp(-rT)]/r, \quad (4)$$

where r is the net annual interest rate, T the structure lifetime, and ΔT the reconstruction/replacement period.

2.2 Annual Failure Probability

The building failure probability is obtained by following the steps shown in the flowchart in Fig. 1.

The location of Cancun is shown in Fig. 2. Cancun was selected because of its high wind exposure, and the building use was a hotel, because the main income for Cancun comes from the tourist sector, and because the large losses experienced, especially by the tourist sector, when the hurricane Wilma hit Cancun [1].

The wind hazard curve, which follows a Gumble distribution as above mentioned, has the form:

$$F_V(v) = \exp(-\exp(-a(V - u))) \quad (5)$$

where V is the maximum wind velocity, and the parameters: $a = 0.03$ and $u = 60.03$ are obtained from the wind

velocities reported, 200 and 250 kph, for the return periods = 50 and 200 years, respectively.

The resulting curve is shown in Fig. 3

1. By performing a series of building response analyses, relationships between the maximum moment and the maximum wind velocity, and between the maximum shear force and the maximum wind velocity, are obtained for the critical sections of the building. For the considered building, it was found that the maximum bending moment governs the response.

The wind load model is based on [28]:

$$F_i = 0.0048C_i^P(V^2)A_i \quad (6)$$

where C_i^P is the pressure coefficient for the node "i", V the wind velocity, and A_i the tributary exposed area for node "i".

2. Then, a simple Monte Carlo simulation process is performed by generating random maximum wind velocities with a Gumble distribution. The maximum bending moment and maximum shear force are calculated for each trial, using the relationships described at the step 1.
3. Two connections (bolted and welded) are proposed as alternatives, and the force at each critical point (critical bolt for the bolted and critical point for the welded one) is calculated in terms of the maximum forces at the joint. The resistance is considered as a lognormal variable and the nominal strength is taken as the mean value and a coefficient of variation of 0.1 is taken from the literature [29].
4. The performance function g is the difference between the resistance R_b (bolted connection), o , or R_w (welded connection) and the maximum acting force R . A combination of shear force and bending moment characterizes the connection critical limit state. A-325 N bolts and 70EXX electrodes are considered for the bolted and welded connection, respectively.
5. The connection failure probability is calculated as the ratio between the number of trials (10000) where the function g is negative or zero, and the total number of trials.

For the building overall failure probability, the failure mechanism is assumed as the occurrence of beams failure on the first three levels, (at the right hand side bay when the load is assumed to act from left to right, and the opposite when it is considered to act from right to left), which involves the failure at six connections (both ends of each beam). Therefore, the building failure probability is calculated by multiplying the six connection failure probabilities.

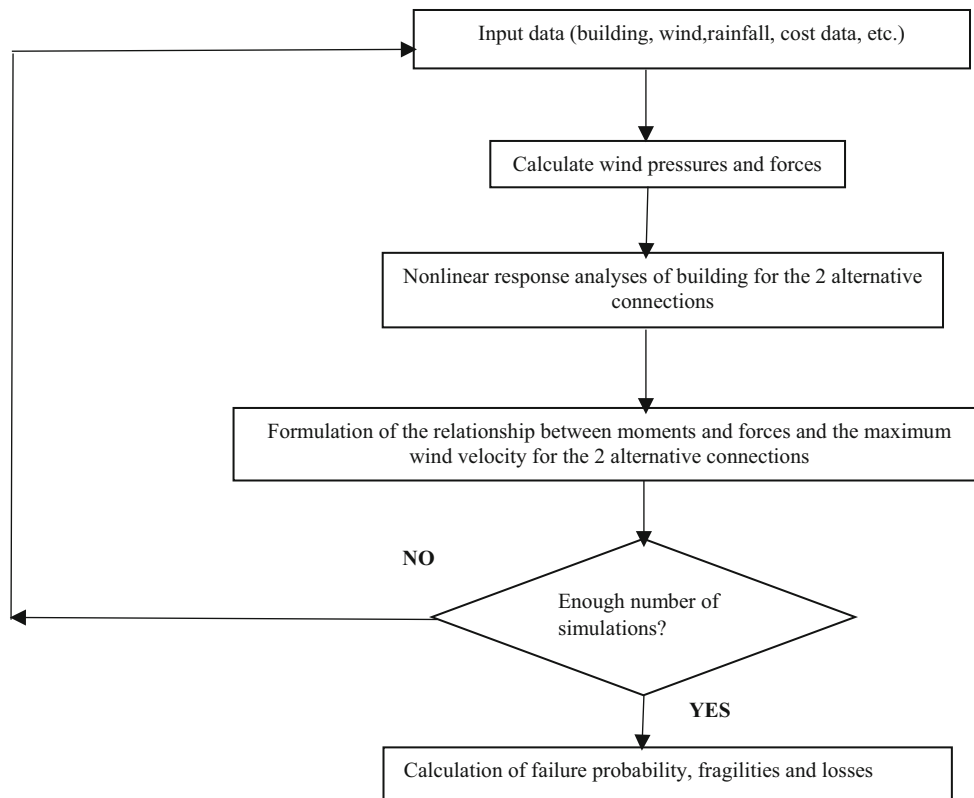
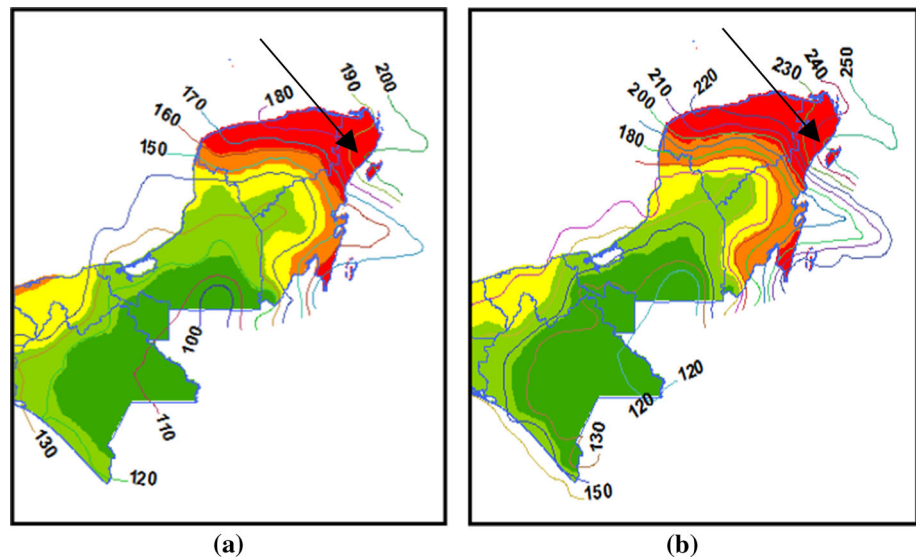


Fig. 1 Flowchart of the proposed procedure

Fig. 2 Location of Cancun and maximum wind velocities (kph) for return periods of **a** 200 and **b** 50 years



A series of preliminary building response analyses were performed to identify the critical frame and critical joint into the building. The combination of bending moment plus shear force was the governing demand as all the connections were designed to avoid local and lateral buckling. In addition, all the member cross sections were designed as compact sections with sufficient lateral support and shear failure modes were also avoided.

The wind pattern, pressure coefficients, and equivalent forces were calculated by the following current design recommendations [30, 31].

A detailed finite-element model of the alternative connections is used to assess, in terms of critical stresses, the performance of the connections under the forces resulting from the frame analyses which, in turn, responded to the scenario maximum wind velocities [32]. These responses

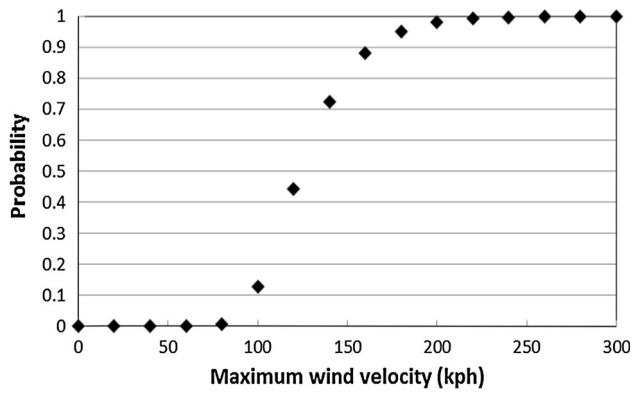


Fig. 3 Wind hazard curve for Cancun

were used to calculate the connection failure probability. Figures 6 and 7 show the bolted and welded connections, respectively.

To develop the limit state function for the governing failure mode of the bolted connection, equivalent forces were obtained in terms of the acting bending moment. A similar development is made for the welded connection.

In addition, from a series of parametric frame analyses, for scenario maximum wind velocities, a relationship between maximum moments and wind velocity is obtained.

The performance functions, for bolted and welded connections, are:

$$g_b = A_b f_{vb} - F_b \tag{7}$$

$$g_w = A_w f_{vw} - F_w \tag{8}$$

where A_b and A_w are the effective bolt and welding areas, f_{vb} and f_{vw} the shear bolt and welding stress (random uniform), and F_b and F_w the acting forces due to the wind demand on the critical bolt and welding point. Monte Carlo simulation techniques were applied to calculate the connection failure probability (RN are uniformly distributed random numbers, M is the maximum moment, T the tension force at the connection, f_{vb} the random shear resistance stress for bolts, g_b is the performance function, R_b the bolt resistant force, and IF is an indicator of failure = 1 if $g < 0$).

Finally, by considering the global failure mechanism as the failure of six connections (both ends of the three beams at the first three levels, right bay of the building), the building failure probability is calculated as:

$$P_f = P_f(\text{Both_joints_for_beams_levels_1_2_3_right_bay}) \tag{9}$$

$$P_f = \prod_{i=1}^6 P_f(\text{Connection_}i). \tag{10}$$

2.3 Loss Analysis

As partial damages may occur during a hurricane, without having the building collapse necessarily, the losses for

lower damage levels need to be considered. The loss, for lower damage levels, requires the cost estimation of typical damages on façades, partial loss of contents due to the potential water infiltration, and partial business interruption as a consequence of the repair works.

The loss L_p , expressed as a percent of the total loss L_T , is calculated as:

$$L_p = [P_1(\text{FC}) + P_2(\text{CC}) + P_f(\text{BC} + \text{BIC})] / L_T \tag{11}$$

where FC is the cost of façade, CC the cost of contents, BC the building cost (without façade), BIC the loss due to business interruption, P_1 and P_2 the occurrence probabilities of façade damage, obtained from reported fragility curves [26], and water infiltration (described in the next paragraph), and L_T the total loss which involves the whole building cost and the business interruption cost.

In addition, the loss of contents was estimated under the following assumptions: the occurrence probability of content loss is the product of the conditional occurrence probability of rainfall given a wind velocity times the occurrence probability of these wind velocity. The conditional rainfall intensity is obtained from the percent measure of expected rainfall intensity conditional to a wind velocity (Eq. 12), obtained from the literature for normal correlated variables, and calculated from a sample of recently recorded hurricanes and the correlation coefficient obtained between the wind velocity and rainfall intensity of these records:

$$E(r | v) = \sigma_r + \rho \sigma_r (r - \mu_r) / \sigma_v \tag{12}$$

where r and v are rainfall intensity and wind velocity, and μ , σ , and ρ are mean value, standard deviation, and the correlation coefficient.

It is recognized that other factors, like debris impact on the building façade or windows, may influence certain kind of damage. However, as this factor requires the consideration of the modeling of variables, like the generation of debris on surrounding constructions and the wind direction, this is not considered in the current formulation.

3 Illustration for the Studied Building

3.1 Failure Probability

A regular steel framed building was analyzed under lateral loads calculated from the typical wind patterns at Cancun, Mexico (a strong winds zone in the Mexican Atlantic Coast), by prescribing six maximum wind velocities. The building has ten stories and Fig. 4 shows the plan and elevation of the typical frame. This frame is designed according to the current code specifications [30, 31] and

Fig. 4 Plan and elevation of typical frame for ten story building

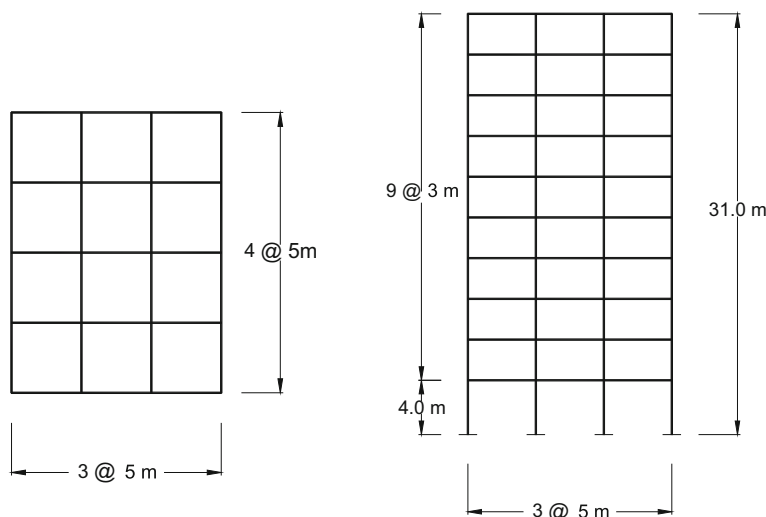


Table 1 Cross sections of considered building

Columns (levels 1, 2)	W18X76
Beams	W14X53
Columns (levels 3–10)	W18X71

recommendations [28], and the cross sections are shown in Table 1. Local buckling and shear failure modes were avoided.

Table 2 contains the dead and live loads used for the considered building, obtained from usual practices and the corresponding code specifications [30]. The material of the building is steel A-36.

The relationship between maximum moments and wind velocity, for the 10 stories building, is shown in Fig. 5. As described in the step 1, Sect. 2.2, the graph of the moments was calculated as the building maximum response at the critical joint under the specified maximum wind velocity. The curve has the purpose to strongly reduce the effort to simulate the maximum response because, instead of the calculation of the building nonlinear response in each of the 10,000 trials, the relationship is assessed with the consequent time saving to obtain a similar result.

Table 3 shows a small sample of the simulation process described in Sect. 2.2, for the structure whose characteristics are detailed here. The process starts with the generation of random numbers, uniform, and Gumbel, to calculate the maximum wind velocity that excites the building and, with that velocity and with the previously obtained relationship between moment and wind velocity, the maximum moment is calculated. In addition, the maximum force at the most stressed bolt is calculated and, with a second uniform random number, the resistance is simulated. Finally, the limit state g is assessed and the

Table 2 Dead and live loads for considered building

Roof level (kg/m ²)	
Dead load	450
Live load	70
Total	520
Other levels (kg/m ²)	
Dead load	486
Live load	90
Total	576

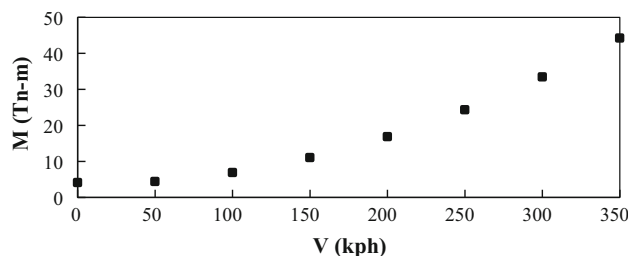


Fig. 5 Maximum moments vs: wind velocity for joints at first 2 levels, ten story building

indicator is assigned a value 1 if the force exceeds the resistance.

The bolted connection consists of four angles $6'' \times 4'' \times 3/4''$, 1 on the top beam flange, 1 at the bottom beam flange, and 2 at the sides of the beam web and 25 A325 $3/4''$ bolts. Figure 6 shows one of the bolted connections.

The critical joint was analyzed for both types: the bolted and welded connections, and a relationship Eqs. (14–16) between the maximum moment, due to the wind loading, and the maximum forces at the critical bolts is obtained:

$$T(d + 4.5'') + T''(d) + T'(2s) = M \tag{13}$$

Table 3 Sample of Monte Carlo simulation for the failure probability of the bolted connection

RN ₁	V (kph)	M (tn-m)	F _{max} (tn)	RN ₂	R _b (tn)	IF
0.83	116.1	5.3	3.6	0.49	5.83	0
0.72	98.1	4.5	3.0	0.72	10.91	0
0.08	29.9	2.6	1.8	0.32	3.72	0
0.67	91.0	4.2	2.8	0.66	9.01	0
0.03	20.0	2.5	1.7	0.03	0.99	1
0.20	44.4	2.9	1.9	0.53	6.54	0
0.70	95.7	4.4	2.9	0.52	6.29	0
0.31	55.4	3.1	2.1	0.34	3.94	0
0.73	98.5	4.5	3.0	0.04	1.06	1
0.22	46.6	2.9	1.9	0.95	34.17	0
0.01	8.3	2.4	1.6	0.25	3.09	0

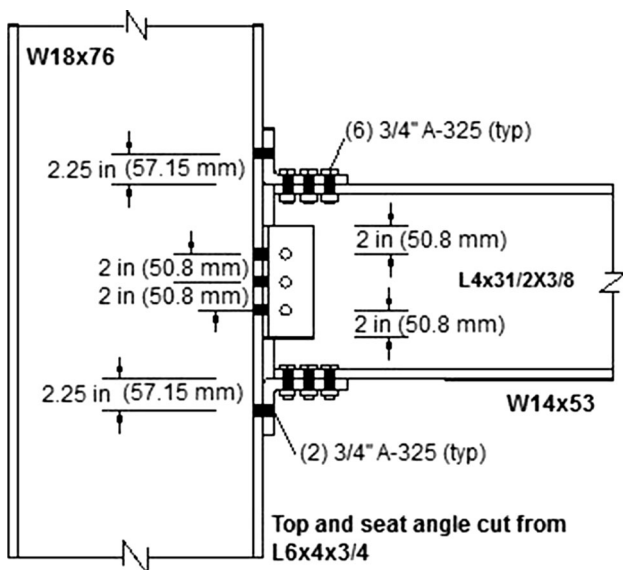


Fig. 6 Bolted connection for critical joint at the three first levels

where d is the beam depth (in this case 14"), s the distance from the beam top flange to the upper bolts centroid (in this case 2.25"), M the demand bending moment, and T the tension force at the top bolts. By assuming a linear distribution of forces:

$$T = M(d/2 + 2.25") / [2(d/2 + 2.25")^2 + d^2/2 + 2s^2]. \tag{14}$$

In addition, the shear force acting at the joint produces a direct shear force at the bolt, which was applied to the same bolts, generating a resultant force R , Eq. (16). If the shear force at the joint, V_f , is resisted by 8 bolts, the tension–shear interaction produces:

$$R = \sqrt{T^2 + (V_f/8)^2}. \tag{15}$$

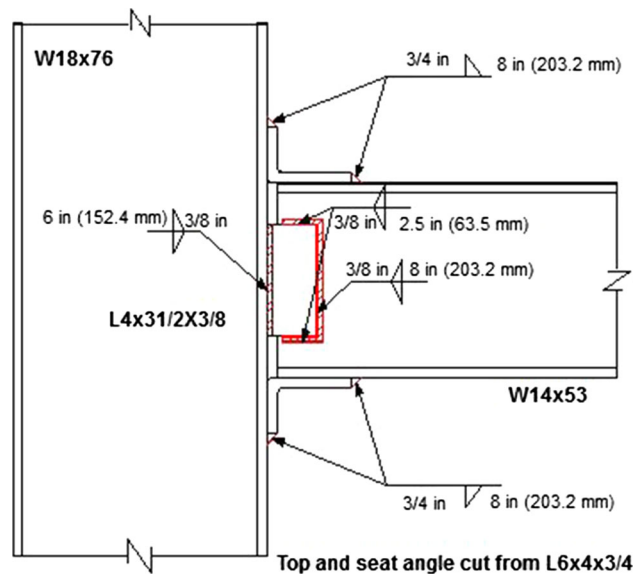


Fig. 7 Welded connection for critical joint at the three first levels

Similarly, for the welded connection, the demand tension force at the critical point of the top weld fillet is:

$$T = M(d/2 + 4") / [(d/2 + 4")^2 + (2s/3)^2]. \tag{16}$$

The tension–shear interaction effects, and the consideration that the horizontal fillets take 1.5 times the force for the vertical fillets, produce a resultant force:

$$R = \sqrt{T^2 + (V_f/A_v)^2}. \tag{17}$$

The welded connection consists of 2 “C” shaped fillets joining the beam web to 4" × 3 1/2" × 3/8" angles, at both sides of the beam web, as shown in Fig. 7. The maximum force on the welding critical point is compared to the welding resistance to assess the connection failure probability.

Figure 8 shows the model used to calculate the forces on the bolted connection, as a consequence of the acting moment. P_{uf} is the ultimate load at the beam flange obtained from the ultimate moment M_u , and the ultimate vertical reaction R_u .

Where A_v is the effective shear area of the horizontal and vertical fillets:

$$A_v = (2L_h \times 1.5 + 2L_v)t(0.7071), \tag{18}$$

where L_h and L_v are the lengths of the horizontal and vertical fillets, respectively, and t is the weld thickness.

Finally, applying Eqs. (9) and (10), the building failure probability for connections bolted and welded is, respectively:

$$P_f B^b = (0.27)^2 (0.28)^2 (0.49)^2 = 0.0014 \tag{19}$$

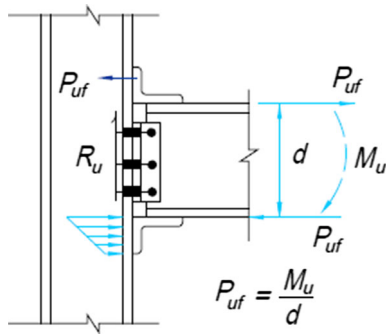


Fig. 8 Model to calculate the forces due to the acting bending moment

$$P_f B^w = (0.238)^2 (0.258)^2 (0.182)^2 = 0.00012. \quad (20)$$

3.2 Expected Life-Cycle Cost for Several Failure Costs

The expected life-cycle cost of alternative buildings with different connection types, under the same wind hazard, is used as a criterion to set judgement to select the connection types. This cost includes, as mentioned in Sect. 2.1, the initial and future damage costs. The future damage cost is updated to present value and the damage consequences include the building components that are damaged, the loss of contents, and the business interruption due to the repair period.

The expected life-cycle cost of each alternative is parametrically studied by modifying the failure costs, to consider several levels of failure consequences. The initial costs are assumed to be, in million USD: $C_i = 4$ (bolted), 7 (welded) and CD_1 is considered to vary from 50 to 200 million USD. See Fig. 9.

It is observed that for failure costs, CD_1 , lower than 100 million USD, the bolted connection is the most cost effective solution, whereas, for higher costs, the welded one would be recommendable. This is because, for low

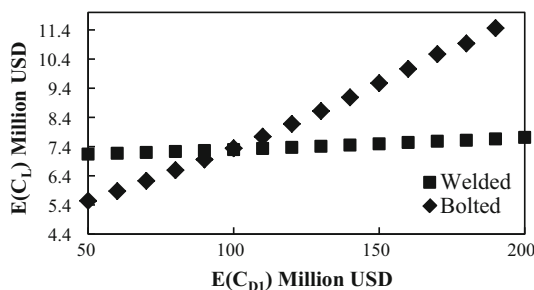


Fig. 9 Comparison of expected life-cycle cost for building with bolted or welded connections

failure consequences, the low initial cost of the bolted connection makes the expected life-cycle cost to be lower than the initial cost of the welded connection. In addition, the reduction on failure probability and, therefore, on the expected failure cost produces a more significant reduction on life-cycle cost for failure consequences over the 100 million USD than under that limit.

3.3 Fragility Curves for Damage Scenarios

Fragility curves for the hotel building are developed for the above described damage scenarios at the precast panels and windows of the hotel building. Assuming that the acting and resistant forces in both: façade panels and screws are lognormal; the damage probability is assessed by applying [27]:

$$\beta = (\ln r_m - \ln r_c) / \sqrt{\zeta_r^2 + \zeta_c^2} \quad (21)$$

where r_m and r_c are the median of resistance and acting force and ζ_r and ζ_c are the dispersion measures of the resistance and load, respectively. The medians for capacities were obtained from reported information by manufacturers [35, 36], whereas for acting loads were calculated from wind pressures over the corresponding areas. The dispersion measures are taken as 0.1 for capacities (façade panel and screws) and 0.3 for the acting pressure, for the different wind velocity scenarios. The damage states were: minor damage level for damage on less than 30% of windows and façade, moderated damage level when between 30 and 60% of windows and façade are damaged and severe damage if more than 60% of these components are damaged. The results are shown in Fig. 10.

It is observed that, as expected, the fragility curves move from left to right as the damage level increases. This produces the effect that the minor damage is more probable for lower wind velocities and that, for the same probability, the damage level increases as the wind velocity increases. This agrees with the shape of the fragility curves developed by FEMA for low rise houses under strong winds [26].

3.4 Loss Curves

If the total cost of damage consists on restoration of façade, doors, and windows, the loss of contents, and the business interruption, a loss curve may be drawn by considering the procedure described in Sect. 2.3.

The cost of façade is taken as 11% of the total building cost, whereas windows and doors are about 2%. According to typical construction costs for hotel in Mexico [37], the cost of the 10 stories building is 4 million USD. Therefore, the total cost of the façade becomes 0.44.

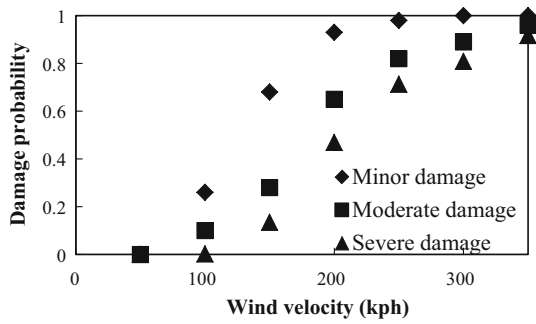


Fig. 10 Fragility curves, for three damage scenarios, for the studied hotel building

The cost of contents (curtains, carpet, beds, and domestic devices) at the hotel room interior is estimated to be 4000 USD per affected room and, if the number of affected rooms is 40, the total cost of damaged contents becomes 0.16 million USD. As the loss of these items depends on the water infiltration due to rainfall and the damage level on windows, the distribution of rainfall intensity, conditional to the occurrence of the hurricane, should be considered. The effect of correlation between the rainfall intensity and the wind velocity is accounted for.

The estimation of the expected loss of contents is made through the simulation of rainfall intensity given a hurricane wind velocity, and it is obtained by multiplying the expected rainfall intensity by the cost of contents. The correlation coefficient is estimated on the basis of a sample of wind velocity and rainfall intensity, for recent hurricanes, in Mexico (see Table 4). The expected rainfall intensity is obtained by multiplying the occurrence probability of the wind velocity by the expected rainfall intensity conditional to the wind velocity (Eq. 12).

In addition, the business interruption is an important cost component and, for the case of the considered hotel, it is obtained as the rental income lost during the reconstruction period.

The income lost is estimated as: the number of rooms (120) times the average accommodation cost per room (200 USD per day) and times an average reconstruction period of 180 days. This makes $BIC = 4.32$ million USD and the expected business interruption cost is obtained by multiplying this loss by the building failure probability:

$$E(BIC) = BIC \times P_f. \tag{22}$$

The total loss L_T is calculated by adding the business interruption cost to the cost of the damaged building components and contents, considered to be 0.68, therefore, 5 million USD.

In addition, mitigated conditions were considered by increasing the anchorage resistance, for façade and windows, by 30%. The losses curves in percent respect to the total loss are shown in Fig. 11.

It is observed that the low-cost mitigation measures have a significant impact on the loss reduction.

4 Discussion of Results

The building use (hotel) and location intended to take into account local practices and the strong wind environment that is common in some areas in Mexico like Cancun. The building response analyses showed, as expected, that the critical joints are located at the ends of the beams at the first level of the building, the ones at the right bay when the wind direction goes from left to right, and the ones at the left bay when the wind goes in the opposite direction. A damage analysis was conducted and the typical damages found on precast façade and windows were reproduced through fragility curves. The fragility curves may be used for a similar buildings located at other sites of the country under other wind hazard environments.

For the wind load and resistance, two random variables are considered: the maximum wind velocity (extreme type I or Gumbel) and the resistant stress for bolts and welding (lognormal distribution). However, the random nature of the water infiltration, which depends on the rainfall intensity, is also accounted for. A novel proposal is the correlation between rainfall intensity and wind velocity, as not all hurricanes produce water infiltration. The expected loss of hotel contents was explicitly calculated including this correlation, because this loss depends on the expected rainfall, which depends on the wind velocity and the correlation between this velocity and the rainfall intensity. In future developments, the change of air pressure at the building interior, once the windows get broken, may be accounted for through fluid dynamics simulations.

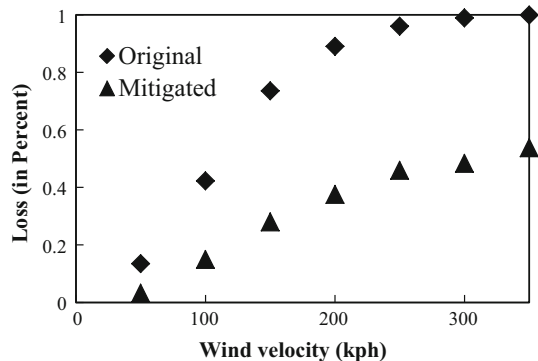
As usually occurs in steel connections, the shear–tension combination governed the limit state of both connection types, where the tension force comes from the bending moment demanded as a consequence of the wind force on the building. Cumulative damage on critical joints is another opportunity to expand the study as many buildings with minor damage may not be repaired in Mexico.

The acting shear force and bending moment due to the wind velocity were randomly generated according to the respective distributions to assess the corresponding limit state and determine the connection failure probability. Here, the coefficient of variation for the wind velocity distribution is taken as a constant; however, in a more detailed model, this coefficient of variation may increase as the mean value of the wind velocity increases.

Another original contribution in this paper is the simplified Monte Carlo simulation process which was developed in a two steps sequence: first, the relationships between maximum wind velocity and acting bending

Table 4 Sample of recent hurricane wind velocities and rainfall intensities recorded during recent hurricanes in Mexico

Year	Hurricane name	Wind velocity (kph)	Rainfall intensity (mm)
1998	Mitch	285	460
2001	Juliette	285	380
2002	Isidore	205	536
2005	Wilma	220	314.3
2006	John	265	275.5
2007	Dean	315	391
2010	Karl	195	105
2010	Alex	175	315.5
2011	Rina	95	234.5
2011	Jova	250	374.4
2011	Arlene	100	348.8
2011	Beatriz	150	222
2013	Manuel	120	381
2013	Ingrid	140	381
2014	Odile	220	250

**Fig. 11** Loss curve for original and mitigated conditions, in percent, for several wind velocities for the studied hotel building

moment and shear force were identified from a series of the frame nonlinear response analyses under prescribed maximum wind velocities. Second, the limit state was appraised for maximum wind velocities generated by following its Gumbel distribution and generating bolt and welding resistances lognormally distributed. At this stage, the bending moment and shear force were obtained, through the before described relationships, in terms of the maximum wind velocity. By doing that, a heavy simulation process involving many structural nonlinear response analyses is avoided because of the deterministic relationship obtained between maximum wind velocity and shear force and bending moment at the critical joint. These deterministic relationships allow for a simplified and faster calculation of joint forces and, therefore, connections failure probability.

The building failure mode was considered to occur when six joints (both ends of the beams at three consecutive levels: from level 1 to level 3) fail provoking a major

collapsed area into the building. This mechanism of partial collapse is more realistic than the rare case of total building collapse.

According to the results, the welded connection was safer than the bolted one, and the cost/benefit balance made through the expected life-cycle cost showed that for buildings with expensive (>100 million USD) cost consequences, the minimum expected life-cycle cost corresponds to the welded connection. On the other hand, less expensive costs of consequences (<100 million USD) make the bolted connection to be the optimal choice. Future research may include the consideration of combined bolts and welding in the same connection and also some bolted, some welded, and some combined connections in the same building.

Given that the initial cost included the cost of labor and the repairs/replacement once the connection is damaged, the higher initial cost of welded connections are justified not only because of the higher installation costs (due to certified workmanship), but also because of the more complicated works implicit for the welding repairs/replacement. The higher quality of the welded connection does not assure that this is the optimal selection, because, although the building may have these connections, the precast façade components may fail and these envelope failures may produce high repair costs and high business interruption losses.

Losses at several damage levels, mild and severe, were estimated for several wind velocities and the loss components of façade loss, loss of contents, and business interruption were considered to represent actual damages during the Wilma hurricane in 2005. Business interruption is very important losses, especially if the hurricane occurs within the high season period, as occurred in the Wilma and Odile hurricanes.

A validation of the formulation is made through the comparison of the calculated losses with those reported for buildings damaged by past hurricanes in Mexico, like Wilma in Cancun and Odile in Baja California. For Wilma, according to the Mexican Association of Insurance Institutions [37], losses raised to about 1.8 billion USD, more than five times the amount payed for the 1985 Mexico City earthquake, 400 claims for hotels, is 4.5 million USD each [1]. This amount is close to the one estimated for the considered hotel building under average damage due to a typical hurricane. Fortunately, human losses are not considered here given that, once the hurricane is close to the building site, evacuation actions may be enforced.

The formulation may be applied to other building types and uses by adapting the building failure modes, limit states, and cost components. The limitations in the correlation structure between wind and rainfall may also be improved. As they are local conditions, the probabilistic distribution for wind and rainfall may change for other sites. The use of passive dissipation energy devices may be encouraged, by studying the building behavior under strong winds.

The proposed procedure can be refined and extended to consider other building structural types, other building heights, hybrid connections (bolted and welded), and other wind hazard levels, among other aspects. In addition, beyond buildings, the wind impact on clean energy facilities, like solar farm and aerogenerator systems, requires additional study. Further research may also provide insights to the problem of optimal repair strategies and the connection degradation in existent steel buildings.

5 Conclusions and Recommendations

A simple procedure, to explicitly assess and compare the cost-effectiveness of bolted and welded connections, has been proposed for a regular steel building under strong wind hazard in Mexico. The formulation includes the overall building safety but also envelope damages.

The procedure includes the calculation of connection and building reliability, and, for the studied case, the welded connection may be recommended for expensive (more than 100 million USD) expected losses, whereas the bolted one is suitable for the less expensive ones. The initial and failure costs were included and the study showed that an expensive connection, like the welded one, not necessarily warranties a lower expected life-cycle cost, as the envelope (facades or windows) may have expensive damages.

The shear–tension stress combination governs the limit states for the connections and, under the consideration that the building fails when six critical connections fail. The building failure probabilities were 1.4×10^{-3} and

1.2×10^{-4} for the building with bolted and welded connections, respectively. It was shown that, although these building failure probabilities are within acceptable margins, the envelope damages produced high losses (material loss and business interruption loss).

The correlation between rainfall intensity and wind velocity was included for the expected losses calculation through the expected loss of contents, which was obtained in an explicit way. In the future, the loss of contents model may be improved by including a fluid dynamics simulation to model the change of air pressures once the windows get broken.

Damage costs on façade and windows, and the business interruption loss, were calculated in an explicit way. All the losses were calculated in terms of expected value; for future research, uncertainty measures may be used to derive margins or intervals to express the variability around the mean values.

Mitigation measures, like improving the anchorage resistance of façade and windows, help to drastically reduce the expected losses. Cost–benefit analyses showed that low-investment measures strongly reduce the expected cost of damages and a campaign of efforts; between government, owners and insurance companies may lead towards an overall improvement of hotels and buildings located on zones with high wind hazard in Mexico.

Further research may provide more robustness, and extend the criteria, to consider other structural systems, other failure modes, building heights, and other wind hazard levels, among other aspects. In addition, other infrastructure facilities, such as bridges, solar farms, and wind-energy generators, may be studied by extending the current formulation.

It is recommended to extend the procedure to consider other types of connections, the contribution of nonstructural elements and the application to select optimal connections for repair of existent buildings. Current wind design codes may be updated by extending the current formulation to cover all kinds of facilities and levels of wind hazard in Mexico.

Acknowledgements The scholarship provided by Consejo Nacional de Ciencia y Tecnología, Mexico, to the second author, to do his master degree, is acknowledged.

Compliance with ethical standards

Funding No funding information is available.

References

1. Avelar FCE (2006) Daños ocasionados por el huracán Wilma en Cancún (in Spanish). Procs XV Congreso Nacional de Ingeniería

- Estructural, Puerto Vallarta, Jalisco. http://www.smie.org.mx/SMIE_Articulos/co/co_14/te_08/ar_11.pdf
2. Murià Vila D (2015) El huracán Odile y sus efectos en la infraestructura del sur de la península de Baja California (in Spanish), Serie Investigación y desarrollo 696:303 (Mexico, D. F)
 3. Tremblay R, Filiatrault A, Timler P, Bruneau M (1995) Performance of steel structures during the 1994 Northridge earthquake. *Can J Civ Eng* 22(2):338–360. doi:10.1139/195-046
 4. Hajjar JF, Leon RT, Gustafson MA, Shield CK (1998) Seismic response of composite moment-resisting connections. II. Behavior. *J Struct Eng Am Soc Civil Eng* 124(8):877–885. doi:10.1061/(ASCE)0733-9445(1998)124:8(877)
 5. Adey BT, Grondin GY, Cheng J (2000) Cyclic loading of end plate moment connections. *Canadian J Civil Eng* 27(4):683–701. doi:10.1139/199-080
 6. Madasamy C, Tyan T, Faruque O, Wung P (2003) Methodology for testing of spot-welded steel connections under static and impact loadings. SAE Techn Paper 2003-01-0608. doi:10.4271/2003-01-0608
 7. Hadianfard MA, Razani R (2003) Effects of semi-rigid behavior of connections in the reliability of steel frames. *Struct Saf* 25(2):123–138. doi:10.1016/S0167-4730(02)00046-2
 8. De Lima ROL, Da Silva LS, Vellasco PCG, Andrade SAL (2004) Experimental evaluation of extended endplate beam-to-column joints subjected to bending and axial force. *Eng Struct* 26:1333–1347. doi:10.1016/j.engstruct.2004.04.003
 9. Castiglioni Carlo A, Mouzakis Harris P, Panayotis Carydis GR (2007) Constant and variable amplitude cyclic behavior of welded steel beam-to-column connections. *J Earthquake Eng* 11(6):876–902. doi:10.1080/13632460601188027
 10. RCSC (2009) Specification for structural joints using high-strength bolts. Res Council Struct Connect
 11. Muir L, Hewitt Ch. M (2009) Design of Unstiffened Extended Single-Plate Shear Connections. *Eng J* second quarter, pp 67–79. <http://www.larrymuir.com/Documents/Design%20of%20Unstiffened%20Extended%20Single%20Plate%20Shear%20Connections.pdf>
 12. Blaney C, Uang C-M, Kim D-W, Sim H-B, Adan SM (2010) Cyclic testing and analysis of retrofitted pre-northridge steel moment connections using bolted brackets. SEAOC 2010 Convent Proceed
 13. Bruneau M, Uang Ch/M, Sabelli R (2011) Ductile design of steel structures. 2nd edn. McGraw Hill Professional, New York
 14. Cao W-G, Zhai Y-C, Wang J-Y, Zhang Y-J (2012) Specification for structural steel buildings. Zhongguo Gonglu Xuebao (China J Highway Transport) 25(2):90–99
 15. Nascimbene R, Rassati GA, Wijesundara K (2012) Numerical simulation of gusset-plate connections with rectangular hollow section shape brace under quasi-static cyclic loading. *J Constr Steel Res* 70:177–189. doi:10.1016/j.jcsr.2011.09.010
 16. Shahidi F, Nateghi-Alahib F, Shahidic F (2013) Non-linear behavior of new (FSFN) moment resisting connections in comparison to the existing KBB connections in steel frames. *Int J Eng (IJE) Trans A Basics* 26(10):1119–1134. doi:10.5829/idosi.ije.2013.26.10a.03
 17. Öztekin E (2015) Investigation of reliabilities of bolt distances for bolted structural steel connections by Monte Carlo simulation method. *J Eng Sci Pamukkale Univ.* doi:10.5505/pajes.2015.29981
 18. Wang K, Yuan SF, Cao DF, Zheng WZ (2015) Experimental and numerical investigation on frame structure composed of steel reinforced concrete beam and angle-steel concrete column under dynamic loading. *Int J Civil Engineering* 13(2):137–147. doi:10.22068/IJCE.13.2.137
 19. Okazaki T, Engelhardt MD, Hong J-K, Uang CM (2015) Improved link-to-column connections for steel eccentrically braced frames. *J Struct Eng.* doi:10.1061/(ASCE)ST.1943-541X.0001041
 20. Skalomenos K, Inamasu H, Shimada H, Kurata M, Nakashima M (2017) Experimental investigation of steel braces installed with intentional eccentricity using gusset plate connections. 16th World Conference on Earthquake Engineering 188. <https://infoscience.epfl.ch/record/225285>
 21. De León D, Reyes Alfredo, Yu Ch (2013) Probabilistic assessment of connections for steel buildings on seismic zones. *J Constr Steel Res* 88:15–20. doi:10.1016/j.jcsr.2013.04.003
 22. Herning G, Garlock MEM, Vanmarcke E (2011) Reliability-based evaluation of design and performance of steel self-centering moment frames. *J Constr Steel Res* 67:1495–1505. doi:10.1016/j.jcsr.2011.03.023
 23. Rosenblueth E (1986) Optimum reliabilities and optimum design. *Struct Saf* 3:69–83
 24. Ellingwood B (1994) Probability-based codified design: past accomplishments and future challenges. *Struct Safety* 13(3):159–176. doi:10.1016/0167-4730(94)90024-8
 25. Ellingwood B, Tekie PB (1999) Wind load statistics for probability-based structural design. *J Struct Eng ASCE* 125:453–463. doi:10.1061/(ASCE)0733-9445(1999)125:4(453)
 26. Vickery PJ, Skerlj PF, Lin JX, Twisdale LA, Young MA, Lavelle FM (2006) HAZUS-MH hurricane preview model methodology. II: damage and loss estimation. *Nat Hazards Rev* 7(2):94–103. doi:10.1061/(ASCE)1527-6988(2006)7:2(82)
 27. Ang Alfredo H-S, Tang Wilson H (2007) Probability concepts in engineering planning and design Vol. I - basic principles. 2nd edn, Wiley, New York
 28. CFE (Comisión Federal de Electricidad) (2008) Manual de Diseño de Obras Civiles. Diseño por viento (in Spanish), México
 29. Carril LaBoube y Yu (1994) Tensile and bearing capacities of bolted connections. Center for cold-formed steel structures library. Missouri University of Science and Technology. EUA
 30. Gobierno del DF (2004) Normas Técnicas Complementarias, Normas metálicas (in Spanish) México
 31. American Institute of Steel Construction (AISC) (2011) Steel Construction Manual, 14th Ed., Chicago
 32. López A, De León D, Cordero C (2008) Reliability analysis and vulnerability functions for HV transmission lines and substations structures. International Federation for Information Processing (IFIP), Working Group 7.5, Reliability and Optimization Structural Systems, 2008, Toluca, Edo. de México
 33. Lind NC, Davenport AG (1972) Towards practical application of structural reliability theory. ACI Publication SP-3, 1972, Probabilistic Design of Reinforced Concrete Buildings, 110. Detroit, Mich., pp 63–110
 34. Stahl B (1986) Reliability engineering and risk analysis. Chapter 5 from Planning and Design of Fixed Offshore Platforms. Edited by McClelland, B. and Reifel, M. D. Van Nostrand Reinhold Co. New York, 1986
 35. <http://www.usg.com.mx>. Accessed 13 Sep 2016
 36. <http://www.gpgypsum.com>. Accessed 13 Sep 2016
 37. AMIS (2006) <http://www.interproteccion.com.mx>. Accessed 13 Sep 2016